



ISSN: 0975-833X

RESEARCH ARTICLE

AC IMPEDANCE SPECTROSCOPY AND ELECTRICAL CONDUCTIVITY STUDIES OF $Ba_{1-x}Zr_xTiO_3$

1,2,*Abdelhalim Elbasset, ¹Farid Abdi, ¹Tajdin. Lamcharfi, ²Haj Omari, L., ²Lamiaie Mrharrab and ³Zouhairi Mohammed

¹LSSC Department of Electrical Engineering, Faculty of Sciences and Techniques, University Sidi Mohammed ben Abdelah, Fes, Morocco

²bLPTA, Physics Department, Faculty of Science University Sidi Mohammed ben Abdelah, Fes, Morocco

³Chemistry Laboratory of Condensed Matter (LCMC), FST Fez B.P.2202 Morocco

ARTICLE INFO

Article History:

Received 07th October, 2015

Received in revised form

24th November, 2015

Accepted 12th December, 2015

Published online 31st January, 2016

Key words:

Electrical Properties, Ac Impedance,
Grain Boundary Effect, Conduction Mechanism.

ABSTRACT

The ac impedance and conductivity properties of $BaZr_xTi_{1-x}O_3$ (BZxT) ceramics in a wide frequency range (1kHz-2MHz) at different temperatures have been studied. An ac impedance spectroscopic technique was used to correlate between the microstructure and electrical properties of the compound. The presence of both bulk and grain boundary effect in the compound was observed. The frequency-dependent electrical data were used to study the conductivity mechanism and estimate the activity energy (E_a). An analysis of the electric impedance with frequency at different temperatures has provided some information to support suggested conduction mechanism.

Copyright © 2016 Abdelhalim Elbasset et al. This is an open access article distributed under the Creative Commons Attribution License, which permits unrestricted use, distribution, and reproduction in any medium, provided the original work is properly cited.

Citation: Abdelhalim Elbasset, Farid Abdi, Tajdin. Lamcharfi, Haj Omari, L., Lamiae Mrharrab and Zouhairi Mohammed, 2016. "Ac impedance spectroscopy and electrical conductivity studies of $ba_{1-x}zr_xti_3$ ", *International Journal of Current Research*, 8, (01), 25113-25118.

INTRODUCTION

Some ferroelectric oxides have been the subject of intense research for variety of applications due to their unique ferroelectric (Dhananjai, 1992), piezoelectric and pyroelectric properties. Among many applications, potential applications of ferroelectric materials are in microwave tunable devices such as tunable mixers, delay lines, filters and phase shifters for steerable antennas (Lakshman et al., 1997; Lancaster et al., 1998; Tagantsev et al., 2003; Yadav et al., 2010). The transition temperature and device parameters of the materials can be controlled by adjusting their compositions. In conventional ceramics, Brager (1955) and Kulscar (1956) have shown that zirconia increases the orthorhombic-tetragonal transition temperature in $BaTiO_3$, and slightly lowers the tetragonal-cubic transition. Verbitskaia et al. (1958) have reported that the $BaZrO_3$ addition to $BaTiO_3$ has an effect similar to ZrO_2 , in that it decreases the axial ratio (c/a) of the tetragonal phase, which is also in agreement with the results found by Moura et al. (1989). On the other hand, Armstrong et al. Tsurumi et al., 2002 have also pointed out the effects of

a small addition of ZrO_2 on the microstructure, dielectric properties and in particular, the grain boundary structure of $BaTiO_3$. $Ba(Zr_xTi_{1-x})O_3$ ceramic is obtained by substituting ions at the B site of $BaTiO_3$ with Zr ions. It is reported that BZxT system has high dielectric constant and low loss tangent at the room temperature. Dielectric properties of BZxT ceramics under a high alternative electric field were reported by Tsurumi et al. (Tsurumi et al., 2002). Zhi Yu et al. (Ang et al., 2002) reported the high tunability of $Ba(Zr_{0.3}Ti_{0.7})O_3$ ceramics. Tang et al. (Tang et al., 2004) reported phase transition and the dielectric tunability of $Ba(Zr_xTi_{1-x})O_3$ ceramics, however these authors laid emphases on the diffuse phase transition and relaxor properties of BZxT ceramics, and on the fact that the behavior of BZxT system under DC electric field was not studied carefully and systematically. So it is necessary to study this behavior systemically and find the main factor of affecting its nonlinear properties. In this paper, we choose $Ba(Zr_xTi_{1-x})O_3$ ceramics ($x=0, 0.025, 0.05, 0.075, 0.10, 0.125$ and 0.15) as research objective. The aim of this work is to study the frequency dependence of electrical (permittivity/loss and impedance/conductivity) parameters and to establish correlation between the microstructure and physical properties of the compound.

*Corresponding author: Abdelhalim Elbasset,

LSSC Department of Electrical Engineering, Faculty of Sciences and Techniques, University Sidi Mohammed ben Abdelah, Fes, Morocco.

Experimental methods

BZxT powders were prepared by the sol-gel method. BZr_xTi_{1-x}O₃ solutions were prepared, dried, powdered and calcined at 900°C during 4 hours. The obtained powders were characterized by X-ray diffraction (DRX) and a scanning electron microscope (SEM). Dielectric measure was performed as a function of the frequency from 1 kHz up to 2 MHz. as we have shown in other works (Elbasset *et al.*, 2014).

RESULTS AND DISCUSSION

The XRD analysis (Fig. 1) revealed that BZxT ceramics crystallized into a perovskite structure without the presence of any secondary phase (pyrochlore).

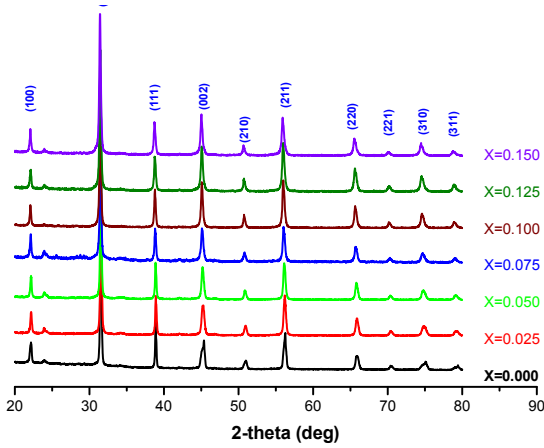


Fig. 1. Room temperature XRD pattern of Ba (Zr_xTi_{1-x})O₃ compounds

The SEM micrographs of ceramic samples (BZxT) sintered at 1100°C for 8 h are shown in Fig.2.

For all samples, we have observed that the fine particles aggregate into grains, which present a quite regular morphology in shape throughout all the composition. As can be seen on in the Table 1, the mean grain sizes of BZxT is about 0.49 to 1.16 μm which. This results indicate that substitution increase the grain size of BZxT. The electrical behavior of the sample was studied over a wide range of frequency and temperature using a complex impedance spectroscopy (CIS) technique. On the other hand the polycrystalline materials usually have grain and grain boundary properties. These contributions can conventionally be displayed in a complex plane plots (Nyquist diagram) in terms of the same formalism:

$$\begin{aligned} \text{Complex impedance: } Z^*(\omega) &= (Z' - jZ'') \\ \text{Complex permittivity: } \epsilon^*(\omega) &= (\epsilon' - j\epsilon'') \\ \text{Complex modulus: } M^*(\omega) &= (1/\epsilon^*(\omega)) = (M' + jM'') \end{aligned}$$

And

$$Z^* = (1/j\omega C_0).M^* \tan\delta = \epsilon''/\epsilon' = Z'/Z'' = M''/M'$$

Where $Z' = |Z|\cos\theta$ and $Z'' = |Z|\sin\theta$

And $\omega = 2\pi f$ is the angular frequency, $C_0 = \epsilon_0 S/e$ is the geometrical capacitance; ϵ_0 is the permittivity of free space, 8.854×10^{-14} F.cm⁻¹, e and S are the thickness and area of the pellet. It is assumed that the impedance date can be represented ideally by an equivalent circuit consisting of two parallel RC elements in series. This circuit is used very widely with materials whose properties are some combination of bulk and grain boundary impedances connected in series. The impedance for this circuit can be described as:

$$Z^* = (R_b^{-1} + j\omega C_b)^{-1} + (R_{gb}^{-1} + j\omega C_{gb})^{-1}$$

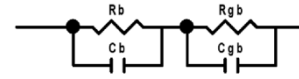


Table 1: Grain size of the BZxT ceramics and fitted parameters of Arrhenius law

x%(Zr)	G. S (μm)	E _a (ev)	f ₀	R _{eq} (10 ⁴ Ω) for 200°C
2.5	0.490	1.1729	13.500	2.776
5	0.600	0.3592	462.733	4.145
10	0.780	2.9904	383.638	4.647
12.5	1.160	1.3317	28.2516	3.254
15	1.40	3.7197	28.3557	2.667

Table 2. Electrical properties of BZxT ceramics simulated using complex formalism of impedance

x% (Zr)	T (°C)	Electrical properties			
		C _{gb} (x10 ⁻¹² Ω)	R _{gb} (x10 ⁷ Ω)	C _b (x10 ⁻¹² Ω)	R _b (Ω)
0%	140	9.74	3.85	-	1850
	160	14.2	4.93	-	1500
	180	9.497	6.697	-	1501
5%	200	7.36	7.27	0,013	1550
	140	17.63	7.068	1.5	1063
	160	13.8	1.029	9.04	1065
	180	17.98	6.697	5.51	1080
7.5%	200	8,65	1.507	7.3	1425
	140	13,7	1.282	-	7127
	160	14,7	2.227	9.5	8510
10%	180	2,85	3.075	14.3	8637
	200	3,74	7,98	2,95	8848
	140	13,1	1.262	5.68	1729
	160	5,97	2.267	10.4	1932
15%	180	4,28	2.051	14.3	5521
	200	7,398	3,72	77.5	6544
	140	9,822	1.242	4.53	442
	160	13,5	1.983	7.87	568
	180	9,61	3.387	6.4	789
	200	7,43	7,78	6,09	1670

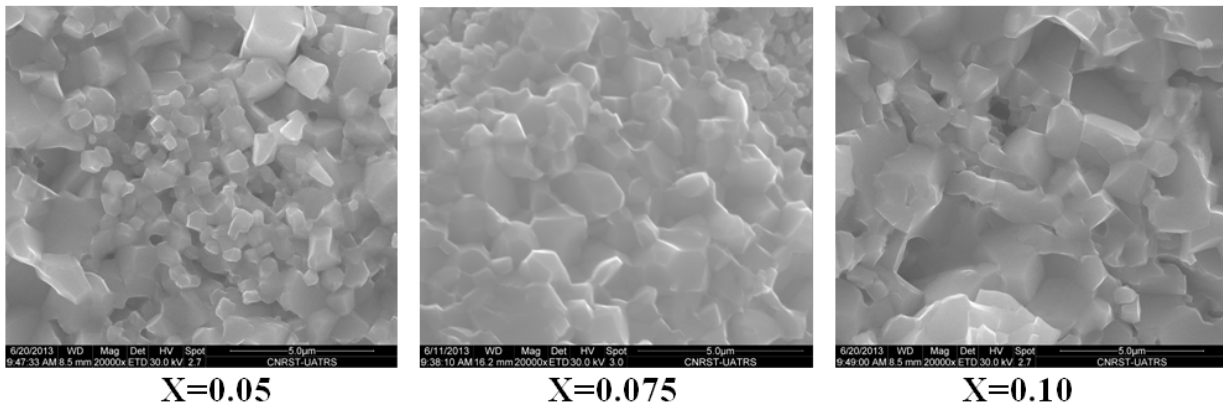


Fig. 2. SEM micrographs of $\text{Ba}(\text{Zr}_x\text{Ti}_{1-x})\text{O}_3$ compounds

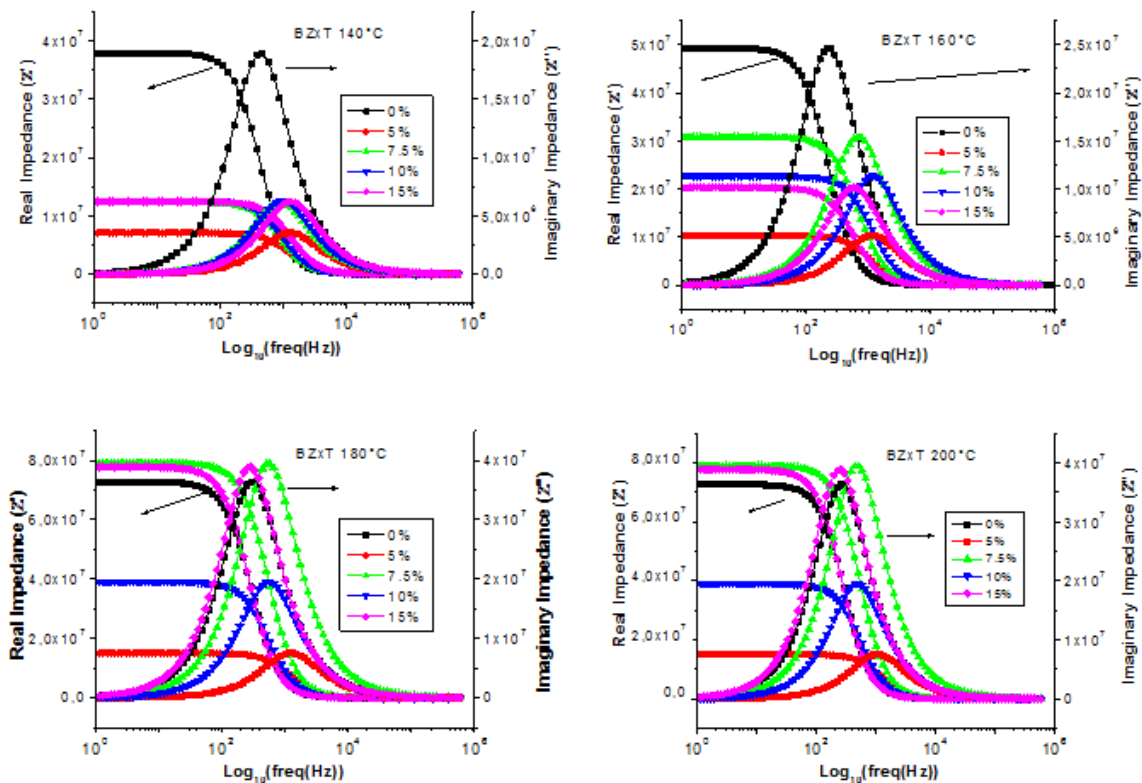


Fig. 3. Variation of real and imaginary part of impedance with frequency of $\text{Ba}(\text{Zr}_x\text{Ti}_{1-x})\text{O}_3$ at various temperatures

The equivalent circuits have been given to simulate the theoretical properties after fitting the complex impedance plots of experiment using commercially available software ZView. The model circuit has been represented by a parallel combination of resistance and Capacitance (C). While in the rest samples it is clear that both the inter-granular (R_b and C_b) and intra-granular (R_{gb} and C_{gb}) impedances are presented in the ceramics, and the simplest appropriate model circuit is a series array of parallel RC elements. The values of fitted parameters have been given in the Table 2. Fig. 3 shows the frequency dependence of the real part (Z') and imaginary part (Z'') of the electrical complex impedance at different temperatures for a proposal samples ($x=0, 0.05, 0.10$ and 0.15%). It is observed that Z' promptly decreases with an increasing frequency from 10^2Hz to 10^4Hz in a fixed $x\%$ in Zr.

In this region, the frequency dependence of Z'' (loss spectrum) shows the peak of resonance at specified value of frequency. The position of the Z'' peak shifts to higher frequency side on increasing $x\%$ in Zr, and then a dispersion of Z'' exist. The width of the peak point (Fig. 3) indicates the possibility of a typical distribution of relaxation times (Raymond *et al.*, 2005). In such a situation, one can determine the relaxation time τ ($= 1/\omega_{\max}$) from the position of the peak. Usually it is possible to find more than one equivalent circuit that fits, numerically, a given data set. In the process of selecting the most appropriate equivalent circuit to represent the electrical properties of a material many difficulties may arise. As there is no priority rule to choose which circuit will perform better, once an equivalent circuit has been selected it is necessary to establish a link between the different parts of the circuit.

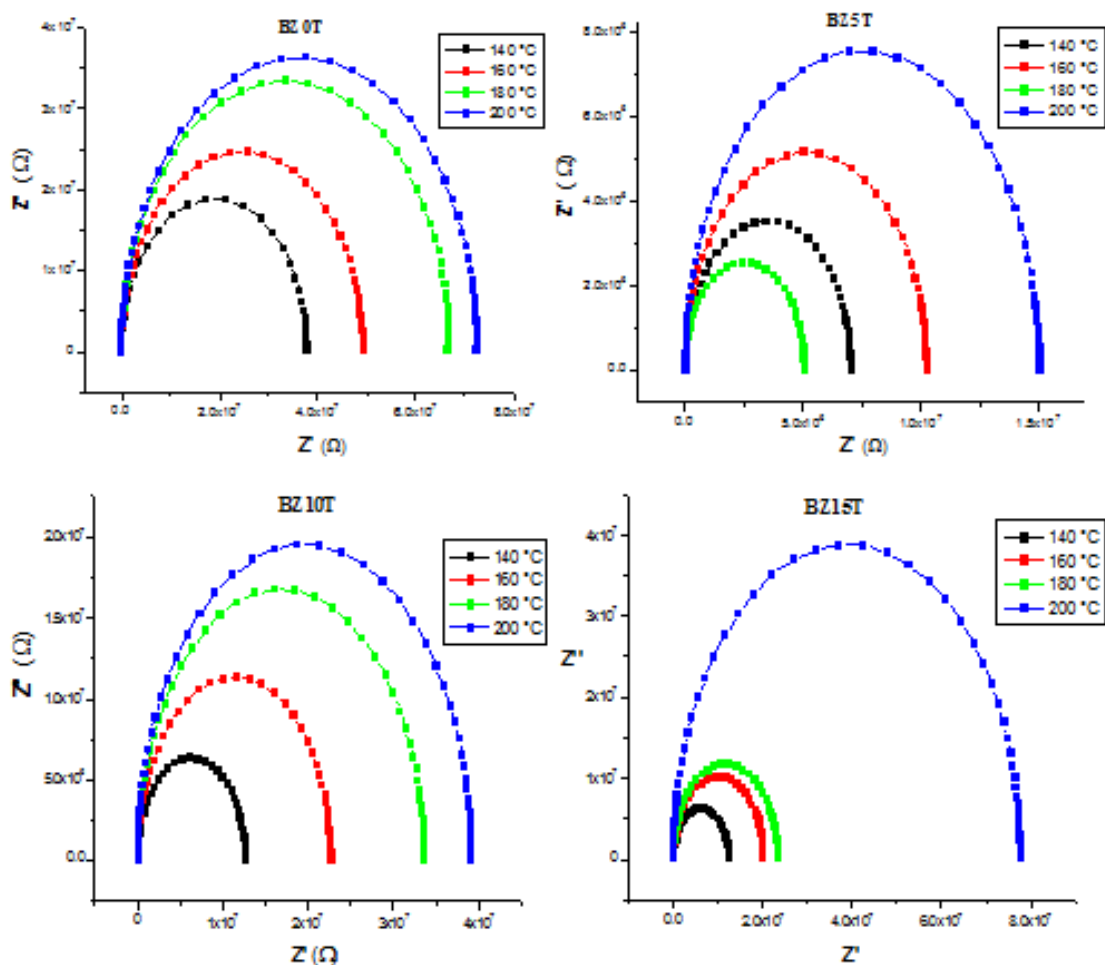


Fig. 4. Evolution of imaginary part of impedance with real part and temperature of $Ba(Zr_xTi_{1-x})O_3$ at various value of x%

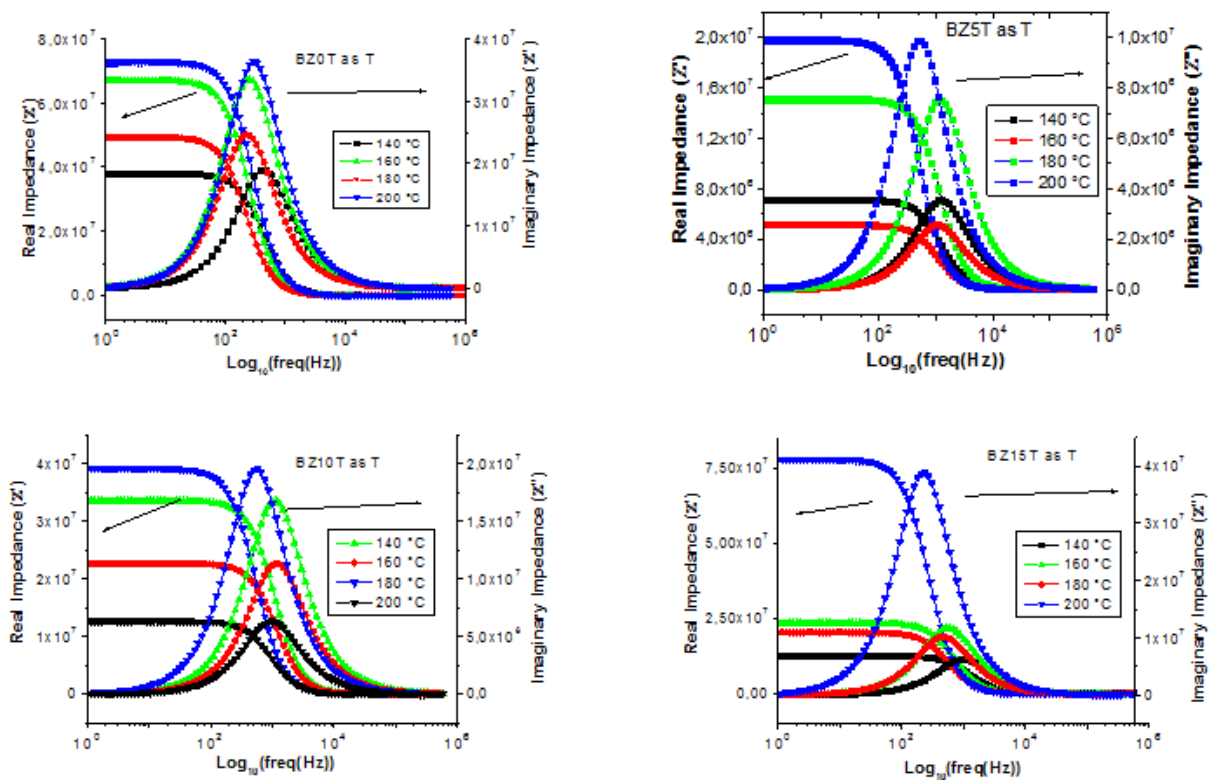


Fig. 5. Variation of real and imaginary part of impedance) with frequency and temperature of $Ba(Zr_xTi_{1-x})O_3$ at various value of x%

In an ideal case, the result of impedance spectroscopy measurements over a wide range of frequencies can be presented by several semicircles in the complex $Z_{Im}-Z_{Re}$ plane. Each semicircle represents the contribution of a particular process (electrodes and contacts, grain boundaries, grain interior) to the total impedance of the sample. Measured values in the form of Nyquist plots are rarely ideal semicircular. Most of the authors describe them as depressed semicircles with their center lying below the x-axis. This phenomenon is called Non-Debye Relaxation (NDR) (Elbasset *et al.*, 2015). Fig. 4 shows the comparable behavior of the impedance and related parameters with increasing temperature from 140 up to 200°C the absence of the second arc in BZxT confirmed that the polarization mechanism corresponds to the bulk effect arising in semi conductive grains. The intercept of the semicircle on the real axis is the bulk resistance (R_b) of the sample.

Fig. 5 shows the variation of real part of impedance (Z') as a function of frequency for all the samples. The nature of variation shows a monotonous decrease in the value of Z' with a rise in the frequency. Larger Z' values at lower frequency and temperature indicated larger effects of polarization. The increase in Z' with rise in temperature also indicates a possibility of the decrease in the ac conductivity with an increase in temperature, which indicate a positive coefficient temperature resistor of the material. We have found that the resistance of the material increase with a rise in temperature.

This behavior of materials is analogous to the positive temperature coefficient of resistance (PTCR) property which is a normal behavior of semiconductor. The merger of the real part of impedance (Z') in the higher frequency domain of all temperatures indicates a possibility of the discharge of space charge as a result of lowering in the barrier properties of the material (Maier, 2003). These results indicate that electrical conduction will decrease with a rise in temperature and the phenomenon is dependent on the release of space charge. This observation may possibly be related to a lack of a restoring force governing the mobility of the charge carriers under the action of an induced electric field at higher temperatures. This behavior supports that as frequency increases; each ion moves a shorter path of electric field until, the electric field changes so rapidly that the ions only “rattle” within the confinement of their potential energy wells. It also indicates the long-range mobility of charge carriers (Behera *et al.*, 2007).

Fig. 5 shows again the variation of the imaginary part of the impedance with frequency (i.e., loss spectrum) at different temperatures. A peak has been observed at higher temperatures which further broadened with a rise in temperature. The trend of the variation of Z'' with frequency is typical of the presence of the electrical relaxation phenomena in the materials which is temperature-dependent. The asymmetric broadening of the peaks suggests the presence of electrical process in the materials with a spread of relaxation time (Bharati *et al.*, 1981). The shifting of peaks indicates that the net relaxation time is decreasing with the increase in temperature. The low frequency side of the peak represents the range of frequency in which charge carriers are mobile over long distances. The higher frequency side of the Z'' peak represents the range of frequencies in which the ions are spatially confined to their

potential wells and the ions can make only short-range motion within the well (Nobre and Langfredi, 2001). The region where peak occurs is indicative of the transition from long-range to short-range mobility with increase in frequency. The behavior of the modulus spectrum is suggestive of temperature-dependent hopping type mechanism for electrical conduction (charge transport) in the system. We have adopted the impedance to study the relaxation mechanism. Here the imaginary impedance (Z'') is plotted as a function of frequency. The peak is observed in the plots corresponding to a relaxation process. The peak height in Z'' against frequency plot is proportional to the resistance of that process and proportional to the capacitance. Here Z' shows a dispersion tending toward Z_∞ , the asymptotic value of Z' at higher frequencies, while Z'' exhibits a maximum Z''_m which shifts to higher frequencies with an increase in the temperature (Fig. 5). The frequency region below the maximum peak Z'' determines the range in which charge carriers are mobile on long distances. At frequency above the maximum peak Z'' , the carriers are confined to potential wells, being mobile on short distances. The frequency ω_m (corresponding to Z''_m) gives the relaxation time τ from the condition $\omega_m\tau = 1$. The capacitance values are calculated at the maximum frequency (f_m) using the relation $Z'' = 2C/\epsilon_0$. The impedance maximum peak shifts to higher frequencies as the temperature increases. It is also observed that the curves are symmetric, implying an exponential behavior of the conductivity relaxation, which suggests the presence of Debye type of relaxation phenomenon (Barik *et al.*, 2007).

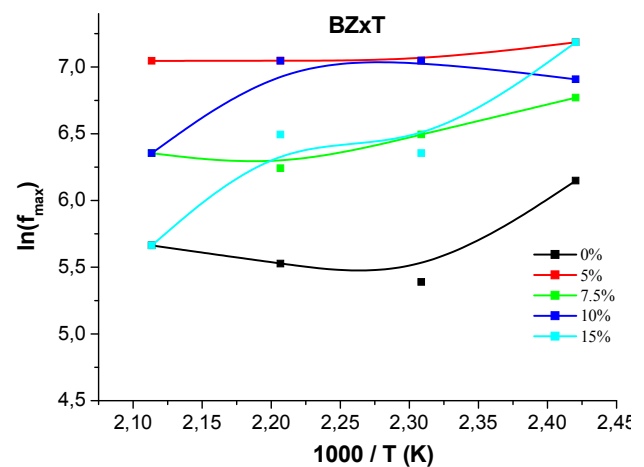


Fig. 6. Variation of relaxation frequency with inverse of temperature ($1000/T$) of $Ba(Zr_xTi_{1-x})O_3$ (for impedance data)

Fig. 6 shows the variation of relaxation time (calculated from loss spectrum) as a function of temperature. The relaxation time in both the cases follows the Arrhenius law given by $\tau = \tau_0 \exp(E_a/K_B T)$ where τ_0 is the pre-exponential factor, K_B is the Boltzmann constant and E_a is the activation energy. The typical pattern suggests a temperature dependent relaxation process with the spread of relaxation time, suggesting an enhancement in the process dynamics (i.e., charge/carrier transport) in the material with a rise in temperature (Victor *et al.*, 2003). Fitting these data to Arrhenius equation allows us to estimate the activation energy E_a , which was found between 0.359 and 3.719 eV. It is clear that the value of the activation energy increases with an increase in Zr concentration.

Conclusion

The phase formation of the sample is confirmed by XRD technique. The presence of space charge polarization at higher temperature arises only due to the mobility of ions and imperfections in the material. A better correlation and understanding of the sample electrical properties with its microstructure in terms of bulk and grain-boundary contribution have been described. The frequency dependence Z' shows that the dynamic processes occurring at different frequencies exhibit the thermal activation process. Imaginary impedance analysis has been carried out to understand the mechanism of electrical transport process, and this indicates a Debye type conductivity relaxation in the material. We have found that the resistance of the material increases with the rise in temperature. This behavior of materials is analogous to the positive temperature coefficient of resistance (PTCR) property which is a normal behavior of semiconductor.

REFERENCES

- Ang, Z., Yu, C., Guo, R. and Bhalla, A.S. 2002. Dielectric properties and high tenability of $Ba(Ti_{0.7}Zr_{0.3})O_3$ ceramics under dc electric field *Appl. Phys. Lett.*, 81, 1285.
- Armstrong, T.R., Margens, L.E., Maurice, A.K. and Buchanan, R.C. 1989. Effect of Zirconia on Microstructure and Dielectric Properties of Barium Titanate Ceramics, *J. Am. Ceram. Soc.*, 72, 605.
- Barik, S.K. Choudhary, R.N.P. and Mahapatra, P.K. 2007. Impedance spectroscopy study of $Na_{1/2}Sm_{1/2}TiO_3$ ceramic, *Appl. Phys.* A 88 217.
- Behera, B., Nayak, P. and Choudhary, R.N.P. 2007. Impedance spectroscopy study of $NaBa_2V_5O_{15}$ ceramic, *J. Alloys Comp.*, 436, 226.
- Bharati, R., Singh, R.A. and Wanklyn, B.M. 1981. On electrical transport in $CoWO_4$ single crystals, *J. Mater. Sci.*, 16, 775.
- Brajer, E.J. 1955. Polycrystalline Ceramic Material U.S. Pat. 2708243.
- Dhananjai, P., Singh, A.P. and Tiwari. V.S. 1992. Developments in ferroelectric ceramics for capacitor applications, *Bull Mater. Sci.*, 15, 391.
- Elbasset, A., Lamcharfi, T., Abdi, F. and Sayouri, S. 2014. Effect of heat treatment time on the dielectric properties of BST. *Adv. Phys., Theor. Applic.*, 30, 45.
- Elbasset, A., Lamcharfi, T., Abdi, F., Mrharab, L. and Sayouri, S. 2015. Effect of Doping with Cobalt or Copper on the Structure of Lead Titanate PT, *Indian Journal of Science and Technology*, 8(12), 56348.
- Kulscar, F. 1956. Fired ceramic barium titanate body, Polycrystalline Ceramic Material U.S. Pat. 2735024.
- Lakshman, P., Rajesh, K.K., Om, P. and Devendra, K. 1997. Evidence of two ferroelectric PTCR components in valence-compensated ceramic system $Ba_{1-x}La_xTi_{1-x}Co_xO$. *Bull. Mater. Sci.*, 20, 933.
- Lancaster, M.J., Powell, J. and Porch, A. 1998. Thin-film ferroelectric microwave devices *Supercond. Sci., Technol.*, 11, 1323.
- Maier, J. 2003. Solid State Ionics. Defect chemistry and ion transport in nanostructured materials: Part II. Aspects of nanoionics 157, 327.
- Moura, F., Simoes, A.Z., Stojanovic, B.D., Zaghete, M.A., Longo, E. and Varela, J.A. 2008. Dielectric and ferroelectric characteristics of barium zirconate titanate ceramics prepared from mixed oxide method, *J. Alloys Comp.* 462, 129.
- Nobre, M.A.L. and Langfredi, S. 2001. Phase transition in sodium lithium niobate polycrystal: an overview based on impedance spectroscopy, *J. Phys. Chem. Solids*, 62, (11) 1999.
- Raymond, O., Font, R., Almodovar, N.S., Portelles, Frequency-temperature response of ferroelectromagnetic $Pb(Fe_{1/2}Nb_{1/2})O_3$ ceramics obtained by different precursors. Part II. Impedance spectroscopy characterization, J. and Siqueiros, J.M. 2005. *J. Appl. Phys.*, 97, 084108.
- Tagantsev, A.K., Sherman, V.O., Astafiev, K.F., Venkatesh, J. and Setter, N. Ferroelectric Materials for Microwave Tunable Applications, J. 2003. *J. Electroceram.*, 11, 5.
- Tang, X.G., Chew, K.H. and Chan, H.L.W. 2004. Diffuse phase transition and dielectric tunability of $Ba(Zr_yTi_{1-y})O_3$ relaxor ferroelectric ceramics *Acta Mater.* 52, 5177.
- Tsurumi, T., Yamamoto, Y., Kakemoto, H. and Wada, S. 2002. Dielectric properties of $BaTiO_3$ $BaZrO_3$ ceramics under a high electric field, *J. Mater. Res.* 17, 755.
- Verbitskaia, T. N., Zhdanov, G.S., Vennertsev, I.N. and Soloviev, S.P. 1958. Dielectric relaxation in laser ablated polycrystalline $ZrTiO_4$ thin films, *Sov. Phys. Crystallogr.* 3, 235.
- Victor, P., Bhattacharyya, S. and Krupanidhi, S.B. 2003. Dielectric relaxation in laser ablated polycrystalline $ZrTiO_4/ZrTiO_4$ thin films *J. Appl. Phys.*, 94, 5135.
- Yadav, K.L. 2010. Structural, dielectric and ferroelectric properties of Y^{3+} doped PZT (65/35), *Adv. Mat. Lett.* 1(3), 259.
